

Aging and Failure of a Polymer Chain under Tension

Harish Charan,¹ Alex Hansen,^{2,3} H. G. E. Hentschel,^{1,4} and Itamar Procaccia^{1,5}¹*Department of Chemical Physics, The Weizmann Institute of Science, Rehovot 76100, Israel*²*PoreLab, Department of Physics, Norwegian University of Science and Technology, N-7491 Trondheim, Norway*³*Beijing Computational Sciences Research Center, CSRC, 10 East Xibeiwang Road, Haidian District, Beijing 100193, China*⁴*Department of Physics, Emory University, Atlanta, Georgia 30322, USA*⁵*Center for OPTical IMagery Analysis and Learning, Northwestern Polytechnical University, Xi'an 710072, China*

(Received 30 July 2020; revised 7 January 2021; accepted 26 January 2021; published 22 February 2021)

The rupture of a polymer chain maintained at temperature T under fixed tension is prototypical to a wide array of systems failing under constant external stress and random perturbations. Past research focused on analytic and numerical studies of the mean rate of collapse of such a chain. Surprisingly, an analytic calculation of the probability distribution function (PDF) of collapse rates appears to be lacking. Since rare events of rapid collapse can be important and even catastrophic, we present here a theory of this distribution, with a stress on its tail of fast rates. We show that the tail of the PDF is a power law with a *universal* exponent that is theoretically determined. Extensive numerics validate the offered theory. Lessons pertaining to other problems of the same type are drawn.

DOI: 10.1103/PhysRevLett.126.085501

Introduction.—The probability of rare events in which materials, devices, or structures fail catastrophically, even when they are expected to remain whole for long *average* times, is a subject of great interest in material physics, in engineering, and in environmental sciences; cf. [1,2], and references therein. The development of techniques and ideas that allow the computation of the probability of rare events is of obvious necessity. In this Letter, we discuss a fundamental problem of this type and maybe one of the simplest, i.e., *a polymer in a thermal bath*; see [3] and references therein. We consider a one-dimensional chain of $N_b + 1$ particles, or beads, interacting with their nearest neighbors with a given potential. The chain is anchored at one end and pulled from the other end using a constant force f . The chain is maintained at temperature T , and the question is, how long will the chain persist until “aging” will result in its breaking, and what is the probability that this collapse will occur at a given time τ ? The breaking time τ is a stochastic variable, since the dynamics at any given temperature induces random fluctuations in the separation of the particles until one (or more) reaches a breaking point. Many studies considered this problem under one guise or another, mainly with the aim of offering a theory for the *mean* breaking time, or the mean rate of breaking $\langle \tau^{-1} \rangle$, where the angular brackets represent an average over many realizations [4–12]. It turns out (and see below) that the *distribution* of breaking rates is not at all sharply peaked, and one should worry about the tail of the distribution that represents rare, but potentially catastrophic, fast rates of breaking (or, *mutatis mutandi*, short times for failure). We are mainly interested in the probability distribution function (PDF) of breaking rates $P(\tau^{-1}; N_b, T, f)$ as a function of

N_b , T , and f . We will show that even in this relatively simple problem there exist relatively high probabilities for rupture at times much shorter than the mean time. In fact, the main result of the Letter is that the PDF of rupture rates exhibits a power-law tail:

$$P(\tau^{-1}; N_b, T, f) \sim [\tau^{-1}]^{-\zeta} \quad \text{for } \tau^{-1} \gg \langle \tau^{-1} \rangle, \quad (1)$$

with a universal exponent $\zeta = 2$ (up to higher-order terms) *independent* of the values of N_b , T , and f . We here show how to calculate ζ theoretically and demonstrate excellent agreement with numerical simulations.

Model.—The positions of $N_b + 1$ beads can be specified by the degrees of freedom $\mathbf{r}_1, \mathbf{r}_2, \dots, \mathbf{r}_{N_b+1}$, where $\mathbf{r} \equiv (x, y)$. The N_b bond stretches are denoted R_1, R_2, \dots, R_{N_b} , where $R_i = |\mathbf{r}_{i+1} - \mathbf{r}_i| - r_e$ with $r_e = 1.54 \text{ \AA}$ being the equilibrium distance between the unstretched bonds. The beads interact via stressed Morse potentials, which for each bond has the form [9]

$$V(R_i, f) = D_e(1 - e^{-\alpha R_i})^2 - fR_i. \quad (2)$$

The total potential of the polymer is the sum $\sum_i^{N_b} V(R_i, f)$ [9]. Thus, the potential is fully specified by three parameters: D_e , α , and f . In our simulations, we used $D_e = 120 \text{ Kcal/mole}$, which is the maximum potential energy of the unstretched Morse potential, $\alpha = 0.5 \text{ \AA}^{-1}$ is an inverse length scale for reaching this maximal stretch, and f is the applied force in $\text{Kcal}/(\text{mole} \times \text{\AA})$. In this Letter, these parameters are the same for every bond, but a richer model can be defined with a distribution of

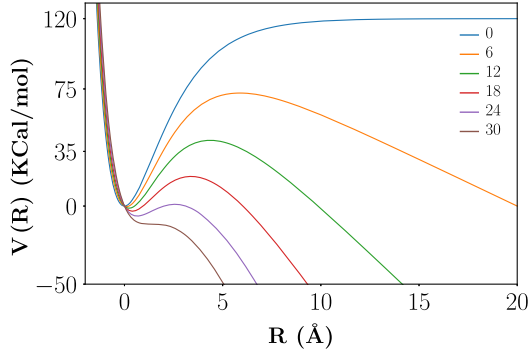


FIG. 1. The strained Morse potential with various values of pulling force f ; see Eq. (2). With the present parameters $f_{\max} = 30$ Kcal/(mole \times Å), any force larger than f_{\max} will result in instant rupture of a bond. Note that R_{eq} increases with f , while R_b decreases until they coalesce at f_{\max} .

parameters. In a stressed Morse potential $V(R, f)$ (see Fig. 1), a potential barrier of size $\Delta(f)$ appears at a distance $R = R_b(f)$. We assume that the chain ruptures if any of the bonds reaches $R = R_b(f)$; no healing phenomena occur in which a chain can reform once it is stretched beyond the peak at $R_b(f)$. The barrier height $\Delta(f)$, the positions of the peak $R_b(f)$, and the minimum of the stretched potential R_{eq} can be calculated as follows:

$$\begin{aligned} \partial V(R, f) / \partial R|_{R=R_b(f)} &= 0, \\ \Delta(f) &= V[R_b(f), f] - V[R_{\text{eq}}(f), f]. \end{aligned} \quad (3)$$

Plugging Eq. (2) into Eqs. (3) then yields analytic forms for $R_b(f)$ and $R_{\text{eq}}(f)$:

$$\begin{aligned} R_b(f) &= -\frac{1}{\alpha} \log \frac{1 - \sqrt{1 - f/f_{\max}}}{2}, \\ R_{\text{eq}}(f) &= -\frac{1}{\alpha} \log \frac{1 + \sqrt{1 - f/f_{\max}}}{2}, \end{aligned} \quad (4)$$

where $f_{\max} = D_e \alpha / 2$. Below, we discuss simulations in which f is not too close to f_{\max} . These are the statistically more interesting situations in which the rupture rates τ^{-1} are widely distributed. For forces too close to f_{\max} , rupture occurs almost instantly and the problem is less challenging. Note that, in general, $\langle \tau^{-1} \rangle$ is increasing with f , becoming singular for f_{\max} .

For a single Morse potential, one can quote the results of transition state theory, which treats the bond breakage as a unimolecular reaction $R_{\text{eq}} \rightarrow R_b$. The *mean* rate for single bond breakage has an Arrhenius form:

$$\langle \tau^{-1} \rangle (R_{\text{eq}} \rightarrow R_b, T, f) = \nu(f) \exp[-\Delta(f)/T], \quad (5)$$

where the ‘‘attempt rate’’ to cross the barrier is given by [9]

$$\nu(f) = \frac{1}{2\pi} \frac{\omega_b(f)\omega_{\text{eq}}(f)}{\sqrt{\omega_{\text{eq}}(f)^2 + 2\omega_b(f)^2}}, \quad (6)$$

with

$$\begin{aligned} m\omega_{\text{eq}}(f)^2 &= d^2V(R_{\text{eq}}, f)/dR_{\text{eq}}^2, \\ -m\omega_b(f)^2 &= d^2V(R_b, f)/dR_b^2. \end{aligned} \quad (7)$$

We will see below that the mean rupture rate, for a single bond or the whole polymer, is not sufficiently informative, since the PDF of the polymer rupture rates is very broad with a power-law asymptotic tail. As said, our aim in this Letter is to go beyond Eq. (5) to compute the tail of the PDF $P(\tau^{-1}; N_b, T, f)$.

Numerical simulations.—To study the rupture of the polymer, we performed molecular dynamics simulations employing LAMMPS [13]. The simulations always begin with the chain of $N_b + 1$ particles connected sequentially, with the first particle being anchored to a wall at position \mathbf{r}_1 . Initially, the chain is thermalized by Langevin dynamics at temperature T , resulting in the chain being folded to a minimum free-energy state. Second, this folded thermalized polymer is then pulled from the last bead by the force f at a constant temperature. In the analysis below, the force f is always larger than the minimal value necessary to stretch the polymer enough to eliminate any long-range interaction between the particles. Temperature in our simulations is measured in degrees Kelvin, but for the purpose of presentation of our results and in the theory discussed below all the parameters are made nondimensional. Temperature is reported in units of De/k_B , where $k_B = 0.0019872041$ kcal/(mole \cdot K) after thermalization, and the constant tensile force f which is applied to the last particle at \mathbf{r}_{N_b+1} is measured in units of f_{\max} . The moment of application of the constant force is declared to be $t = 0$. The simulations are employed to determine the time τ at which the chain breaks. For every ensemble, we normalize the rupture times by the maximal inverse time τ_{\max}^{-1} for that ensemble. Finally, bond stretches are normalized by R_b . A typical simulations for a dimensionless force $f \approx 0.7$ of a chain with 41 beads at dimensionless temperature $T = 0.0109$ is shown in the movie that can be observed in Supplemental Material [14]. During simulations, we prepare typically 4000 independent realizations of the polymer and determine for each the rupture inverse time τ^{-1} . Typical PDFs of τ^{-1} as obtained in simulations are shown in Fig. 3. The data are shown in a log-log plot to stress that the distribution is very wide. There is a high probability to rupture quickly, much quicker than the average rate; the tail of the PDF decays as slowly as a power law. Our aim is now to understand and compute the power-law tail of these distributions.

Theory.—Here, we present a theory to estimate the PDF $P(\tau^{-1}; N_b, T, f)$. We begin with some elementary statistical mechanics. Define the bond partition function as

$$Z_{\text{bond}}(T, f) = \int_0^{R_b(f)} dR \exp[-V(R, f)/T]. \quad (8)$$

We will assume that the moment that any bond reaches R_b the chain breaks instantly and it does not heal. Denote now the cumulative probability $C(R, T, f)$ for a single bond to be stretched any distance $0 < R < R_b$. This is given by

$$C(R, T, f) = \int_0^R dr \exp[-V(r, f)/T]/Z_{\text{bond}}(T, f). \quad (9)$$

To connect this to the rate of rupture, we will assert that the bond that breaks is always the bond that has reached the largest extension among all the bonds. Obviously, such a bond exists in every realization. It does not always break, but, when rupture occurs, it is always due to the breaking of that bond that was maximally extended. Here, we are interested in the situations for which $f < f_{\text{max}}$, meaning that the chain reaches thermal equilibrium and equipartition, much before it ruptures. Denote then the probability that *any* single bond has a length less than R as $P_{<}(R)$ and that it is greater than R as $P_{>}(R)$. Using Eq. (9), we can write

$$P_{<}(R) = C(R), \quad P_{>}(R) = 1 - C(R). \quad (10)$$

For N_b bonds, the probability density that exactly one bond will have length larger than R_{max} is

$$P_1(R_{\text{max}}; N_b, T, f) = \frac{N_b}{Z_1(T, f)} P_{>}(R_{\text{max}}) [P_{<}(R_{\text{max}})]^{N_b-1},$$

$$Z_1(T, f) = N_b \int_0^{R_b(f)} dR P_{>}(R) [P_{<}(R)]^{N_b-1}. \quad (11)$$

Clearly, this result is exact provided that the polymer is thermalized before it ruptures. We reiterate that this condition excludes forces that are too high, since then rupture can take place before thermalization. A typical comparison to numerical simulations is shown in Fig. 2. Not surprisingly, agreement is excellent. Note in passing that for $N_b \rightarrow \infty$ this PDF is expected to converge to one of the canonical functions in extreme value statistics, known as the Weibull distribution [15,16]. Obviously, it is an analytic function with an end point at $R_{\text{max}} = R_b$ where it vanishes. As such, it can be expanded near its end point:

$$P_1(R_{\text{max}}; N_b, T, f) = \alpha(R_b - R_{\text{max}}) \quad \text{for } R_{\text{max}} \rightarrow R_b, \quad (12)$$

with α being the derivative at R_b .

Denote now the breaking rate that we measure in simulations $\tau^{-1}(R_{\text{eq}} \rightarrow R_b; N_b, T, f)$. This is a random variable, and we will be unable to determine analytically

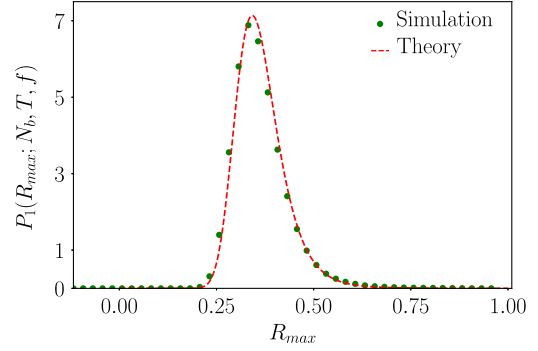


FIG. 2. Comparison between the theoretical PDF for maximal bond extension Eq. (11) and its numerical measurement. Here $N_b = 11$, $T = 0.0072856\dots$ and $f = 0.77$.

its full distribution. Rather, we will aim at the distribution of large rates which is dominated by the probability of bonds to stretch to large distances at short times. The quantity of theoretical interest will be therefore $\tau^{-1}(R_{\text{max}} \rightarrow R_b; N_b, T, f)$. The PDF of our wanted rates for rupture is

$$P(\tau^{-1}; N_b, T, f) = \int_0^{R_b} dR_{\text{max}} P_1(R_{\text{max}}; N_b, T, f) \times \delta[\tau^{-1} - \tau^{-1}(R_{\text{max}} \rightarrow R_b; N_b, T, f)]. \quad (13)$$

Note that the integral is over bond lengths, whereas the δ function is over rates. To perform the integral, we need to relate the two. To do this, we recognize that the rate τ^{-1} which appears in the PDF and in the δ function is arbitrary, and it will be associated with *some* R_{max} , say, $R_{\text{max}} = R^*$, which satisfies the condition

$$\tau^{-1}(R^* \rightarrow R_b; N_b, T, f) = \tau^{-1}. \quad (14)$$

Imagine that we succeeded to determine the relationship $R^* = R^*(\tau^{-1})$. Then, changing variables accordingly, Eq. (13) leads to

$$P(\tau^{-1}; N_b, T, f) = \frac{dR^*}{d\tau^{-1}} P_1(R^*; N_b, T, f). \quad (15)$$

So our task now is to find the Jacobian of the transformation $dR^*/d\tau^{-1}$.

To find this Jacobian, we need to make approximations. First, we assume that the total time for breaking can be written as the sum of the time for reaching R^* during the thermal agitation and then the time from R^* to R_b :

$$\tau(R_{\text{eq}} \rightarrow R^*) + \tau(R^* \rightarrow R_b) = \tau(R_{\text{eq}} \rightarrow R_b). \quad (16)$$

Since we are interested in the rates, we invert this equation in favor of the fast rate going from R^* to R_b :

$$\tau^{-1}(R^* \rightarrow R_b) = [\tau(R_{\text{eq}} \rightarrow R_b) - \tau(R_{\text{eq}} \rightarrow R^*)]^{-1}. \quad (17)$$

Second, we assume that the major source of randomness is in the distribution $P_1(R_{\text{max}})$, which is governed by the thermal agitation. Therefore, *for the purpose of estimating the Jacobian*, the random times appearing in Eq. (17) can be estimated by their means. Thus,

$$\begin{aligned} \tau^{-1}(R_{\text{eq}} \rightarrow R_b; N_b, T, f) &\sim \nu(f) e^{-\Delta(f)/T}, \\ \tau^{-1}(R_{\text{eq}} \rightarrow R^*; N_b, T, f) &\sim \nu(f) e^{[V(R_{\text{eq}}, f) - V(R^*, f)]/T}. \end{aligned} \quad (18)$$

Returning now to Eq. (17), we note that if R^* is close to R_b where the potential has a maximum, we can estimate to second order in $R_b - R^*$:

$$V(R_b, f) - V(R^*, f) = \frac{m\omega_b^2(f)}{2} (R_b - R^*)^2. \quad (19)$$

Using now Eqs. (18) and (19) in Eq. (17) results in

$$R_b - R^* = \sqrt{\frac{2T}{m\omega_b^2(f)}} \left[-\ln \left(1 - \frac{\nu(f) \exp[-\Delta(f)/T]}{\tau^{-1}} \right) \right]^{1/2}. \quad (20)$$

Computing the derivative of R^* with respect τ^{-1} , we end up with

$$\begin{aligned} \frac{dR^*}{d\tau^{-1}} &= \sqrt{\frac{T}{2m\omega_b^2(f)}} \left[-\ln \left(1 - \frac{\nu(f) \exp[-\Delta(f)/T]}{\tau^{-1}} \right) \right]^{-1/2} \\ &\times \frac{\nu(f) \exp[-\Delta(f)/T]}{\tau^{-1} \{ \tau^{-1} - \nu(f) \exp[-\Delta(f)/T] \}}. \end{aligned} \quad (21)$$

Equations (15) and (21) are our theoretical predictions that should be compared with the results of numerical simulations. For $\tau^{-1} \gg \langle \tau^{-1} \rangle$, we find that the Jacobian Eq. (21) goes as

$$\frac{dR^*}{d\tau^{-1}} \propto [\tau^{-1}]^{-3/2} \quad \text{for } \tau^{-1} \gg \langle \tau^{-1} \rangle, \quad (22)$$

up to higher-order terms. On the other hand, combining Eqs. (12) and (20), we find that

$$P_1(R^*; N_b, T, f) \sim [\tau^{-1}]^{-1/2}, \quad (23)$$

again up to higher-order terms. Together, these two factors result in a power-law tail for $P(\tau^{-1}; N_b, T, f)$:

$$P(\tau^{-1}; N_b, T, f) \sim [\tau^{-1}]^{-2} \quad \text{for } \tau^{-1} \gg \langle \tau^{-1} \rangle, \quad (24)$$

up to higher-order corrections. We note that this result is independent of N_b , T , and f as long as the polymer

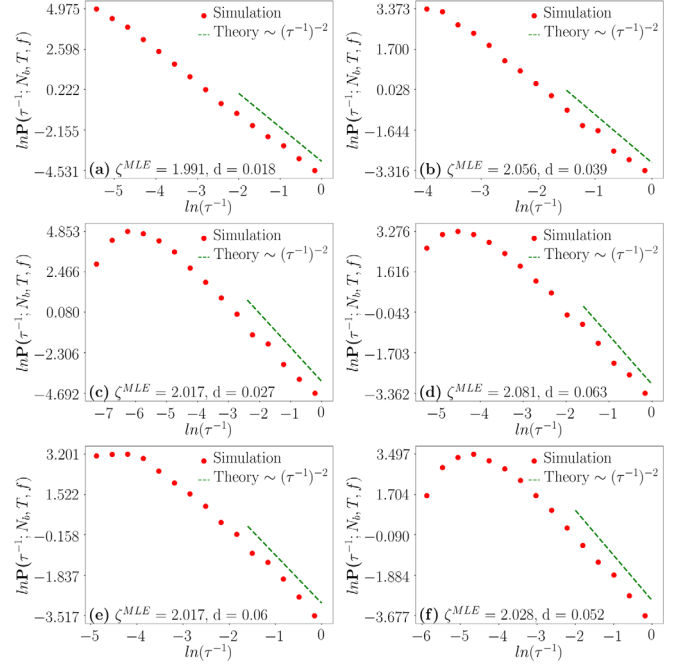


FIG. 3. Comparison of the numerically simulated PDF $P(\tau^{-1}; N_b, T, f)$ to the theoretical prediction of its tail, for six different sets of parameters. We reiterate that τ^{-1} is normalized by its maximum value as found in each case. In dots are the simulations, and in dashed curves are the theoretical prediction Eq. (24). (a) $N_b = 11$, $T = 0.0073$, and $f = 0.77$. (b) $N_b = 21$, $T = 0.0109$, and $f = 0.68$. (c) $N_b = 41$, $T = 0.0146$, and $f = 0.58$. (d) $N_b = 81$, $T = 0.0109$, and $f = 0.63$. (e) $N_b = 161$, $T = 0.0109$, and $f = 0.62$. (f) $N_b = 321$, $T = 0.0109$, and $f = 0.58$. In all panels, we provide the slope computed via the maximum likelihood estimate (MLE) [17] and the Kolmogorov-Smirnov distance (d).

equilibrates before snapping. This is a surprisingly universal result that needs to be compared to simulations.

Comparison of theory and simulations.—In comparing our theory to the numerical simulations, we remember that the former is limited to the tail of the PDF $P(\tau^{-1}; N_b, T, f)$ for $\tau^{-1} \gg \langle \tau^{-1} \rangle$. The actual distribution is normalized, but the theoretical prediction is not. The comparison is presented in Fig. 3 for six different choices of parameters. In particular, we note that the prediction of a power-law tail is very well supported, and the exponent in the power-law tail computed theoretically fits well the tail of the actual normalized distribution as found in the simulations. The agreement between theory and simulations shown in Fig. 3 is typical *as long as the polymer has reached thermal equilibrium before rupture*. We have also considered forces f that are too high for the polymer to equilibrate (not shown here), and, not surprisingly, the excellent agreement exhibited in Fig. 3 disappears. In such cases, also the comparison of the measured $P_1(R_{\text{max}}; N_b, T, f)$ to the theoretical result Eq. (11) as shown in Fig. 2 is no longer favorable.

Summary and discussion.—In summary, we show that the ability to predict the tail of the PDF for fracture rates in the stressed polymer chains, and also in many other similar problems, depends on two ingredients. The first is an identification of the “weakest link,” which in this case is the bond that extends most, denoted above as R_{\max} . A first step of the analysis requires a calculations of the PDF of this weakest link. When the random perturbations are thermal, standard statistical mechanics suffices to compute the PDF. If the random perturbations are of a different sort, their nature and their statistics must be provided in order to achieve this first step. Note that usually the PDF computed in the first step is expected to be of the Weibull type, but this by itself is not sufficient to provide the universal tail. The second step is where our approach appears novel, in determining the rate of failure associated with each value of the maximally dangerous link. In the present example, it is Eq. (20) that provided the necessary relation. In any other problem of a similar type, physical intuition should be exercised again to state the analogous relation. Only the combination of these two steps can provide predictability of the type shown in Fig. 3. In future work, one will need to explore these ideas in more complex models like bundles of polymers, say, of poly-ethylene oxide [11], protein gels [18], and other biological examples; cf. Refs. [19,20]. Also one needs to remember that, under constant strain, results for aging may differ [21].

We thank Eivind Bering and Astrid de Wijn for useful discussions. This work was supported by the Minerva Center for “Aging, from Physical Materials to Human Tissues,” the scientific and cooperation agreement between Italy and Israel through the project COMPAMP/DISORDER, and the Research Council of Norway through its Centres of Excellence funding scheme, Project No. 262644. A.H. thanks the Norwegian-Israeli Research Fund for additional funding.

-
- [1] D. Sornette, L. Knopoff, Y. Y. Kagan, and C. Vanneste, Rank-ordering statistics of extreme events: Application to the distribution of large earthquakes, *J. Geophys. Res. Solid Earth* **101**, 13883 (1996).
 - [2] W. Schutz, A history of fatigue, *Eng. Fract. Mech.* **54**, 263 (1996).
 - [3] R. K. Puthur, Theory of Breaking of a Polymer Molecule Under Tension (2001), <https://shodhganga.inflibnet.ac.in/handle/10603/5998>.

- [4] F. Bueche, Tensile strength of plastics below the glass temperature, *J. Appl. Phys.* **28**, 784 (1957).
- [5] S. N. Zhurkov and V. E. Korsukov, Atomic mechanism of fracture of solid polymers, *J. Polym. Sci.* **12**, 385 (1974).
- [6] P. Hänggi, P. Talkner, and M. Borkovec, Reaction-rate theory: Fifty years after Kramers, *Rev. Mod. Phys.* **62**, 251 (1990).
- [7] T. Doerr and P. Taylor, Breaking in polymer chains. I. The harmonic chain, *J. Chem. Phys.* **101**, 10107 (1994).
- [8] F. Oliveira and P. Taylor, Breaking in polymer chains. II. The Lennard-Jones chain, *J. Chem. Phys.* **101**, 10118 (1994).
- [9] R. K. Puthur and K. L. Sebastian, Theory of polymer breaking under tension, *Phys. Rev. B* **66**, 024304 (2002).
- [10] A. Sain, C. L. Dias, and M. Grant, Rupture of an extended object: A many-body Kramers calculation, *Phys. Rev. E* **74**, 046111 (2006).
- [11] E. Bering and A. S. de Wijn, Stretching and breaking of PEO nanofibres. A classical force field and *ab initio* simulation study, *Soft Matter* **16**, 2736 (2020).
- [12] G. Linga, P. Ballone, and A. Hansen, Creep rupture of fiber bundles: A molecular dynamics investigation, *Phys. Rev. E* **92**, 022405 (2015).
- [13] S. Plimpton, Fast parallel algorithms for short-range molecular dynamics, *J. Comput. Phys.* **117**, 1 (1995).
- [14] See Supplemental Material at <http://link.aps.org/supplemental/10.1103/PhysRevLett.126.085501> for movie of the polymer being stretched from one end and how it responds to thermal fluctuation until it finally breaks.
- [15] S. Coles, J. Bawa, L. Trenner, and P. Dorazio, *An Introduction to Statistical Modeling of Extreme Values* (Springer, New York, 2001), Vol. 208.
- [16] A. Hansen, The three extreme value distributions: An introductory review, *Front. Phys.* **8**, 604053 (2020).
- [17] J. Alstott, E. Bullmore, and D. Plenz, Powerlaw: A python package for analysis of heavy-tailed distributions, *PLoS One* **9**, 1 (2014).
- [18] M. Leocmach, C. Perge, T. Divoux, and S. Manneville, Creep and Fracture of a Protein Gel Under Stress, *Phys. Rev. Lett.* **113**, 038303 (2014).
- [19] U. Seifert, Rupture of Multiple Parallel Molecular Bonds under Dynamic Loading, *Phys. Rev. Lett.* **84**, 2750 (2000).
- [20] Z. Hu, L. Cheng, and B. J. Berne, First passage time distribution in stochastic processes with moving and static absorbing boundaries with application to biological rupture experiments, *J. Chem. Phys.* **133**, 034105 (2010).
- [21] E. Bering, S. Kjelstrup, D. Bedeaux, J. M. Rubi, and A. S. de Wijn, Entropy production beyond the thermodynamic limit from single-molecule stretching simulations, *J. Phys. Chem. B* **124**, 8909 (2020).